



OPEN Age-associated alteration of innate defensive response to a looming stimulus and brain functional connectivity pattern in mice

Célia Bak, Aroha Boutin, Sébastien Gauzin, Camille Lejards, Claire Rampon & Cédric Florian

Innate defensive behaviors are essential for species survival. While these behaviors start to develop early in an individual's life, there is still much to be understood about how they evolve with advancing age. Considering that aging is often accompanied by various cognitive and physical declines, we tested the hypothesis that innate fear behaviors and underlying cerebral mechanisms are modified by aging. In our study we investigated this hypothesis by examining how aged mice respond to a looming visual threat compared to their younger counterparts. Our findings indicate that aged mice exhibit a different fear response than young mice when facing this imminent threat. Specifically, unlike young mice, aged mice tend to predominantly display freezing behavior without seeking shelter. Interestingly, this altered behavioral response in aged mice is linked to a distinct pattern of functional brain connectivity compared to young mice. Notably, our data highlights a lack of a consistent brain activation following the fear response in aged mice, suggesting that innate defensive behaviors undergo changes with aging.

Fear can be defined as an emotion experienced by an individual in the face of danger or threat, and which elicits multiple behavioral responses. Among these, freezing (i.e. total immobility, except for respiratory movements) and escaping behaviors are particularly well conserved through evolution and across species. Indeed, these threat-evoked responses are found in lizards¹, squirrels², crayfishes³, fish^{4,5}, *Drosophila*^{6,7}, birds^{8,9}, mice¹⁰ and in humans^{11,12}. The critical choice between freezing and flight in response to risks of predation appears to be a major criterion in individual's survival. This choice is determined by several factors, including environmental characteristics and threat features^{1,3,13,14}.

In rodents, a variety of setups and environmental stimuli are employed to assess fear behaviors. For instance, painful experiences (e.g. electrical foot-shock), predator odors (e.g. fox urine) or visual cues imitating predators (e.g. looming and sweeping stimuli) are commonly used¹⁵. Two types of fear are mainly studied in rodents: learned fear and innate fear. The *learned fear response* is elicited after the individual has associated a neutral stimulus (e.g. a tone or a context) with an aversive stimulus (e.g. a predator odor or an electrical foot-shock), so that the learned fear is triggered by the neutral element. In contrast, the *innate fear response* requires no prior learning, it is the immediate reaction to the aversive stimulus or threat itself. This innate fear response has been explored in rodents using looming or sweeping stimuli. The looming stimulus mimics the rapid approach of a flying predator, producing flight and/or freezing reactions, while the sweeping stimulus mimics the predator passing above the subject, eliciting only a freezing reaction^{10,16}. The brain structures and circuits underlying the fear-evoked responses to a looming stimulus have been previously explored. Numerous studies have demonstrated the role of the superior colliculus (SC) in regulating these responses. Anatomically, a subset of retinal ganglion cells innervates the SC¹⁷, which is connected to the ventral tegmental area and mediates the innate defensive behaviors elicited by looming¹⁸. Furthermore, the SC contains parvalbumin neurons that project directly to the parabigeminal nucleus (PBGN) located in the midbrain and the lateral posterior thalamic nucleus (LPTN)¹⁹. Interestingly, it was found that the optogenetic activation of the SC-PBGN pathway induces flight followed by a freezing response, while activation of SC-LPTN triggers immediate freezing behavior¹⁹. In addition, the anatomical connection between the SC and the dorsal periaqueductal gray (dPAG) mediates the initiation of escape behavior, as it has been shown by coupling calcium imaging and optogenetic approaches²⁰. Finally, the SC send projections to the ventral midline thalamus²¹ which controls the reaction to visual threats²². The SC is

CNRS, UPS, Centre de Recherches sur la Cognition Animale (CRCA), Centre de Biologie Intégrative (CBI), Université de Toulouse, Toulouse, France. ✉email: cedrick.florian@univ-tlse3.fr

also connected to the locus coeruleus²³ and works in concert with the dorsal raphe nucleus¹⁷. Furthermore, it is well established that the amygdala has a major implication in fear²⁴, as well as in the response to a looming stimulus. Indeed, Salay and collaborators showed an increase of the looming-evoked freezing response when the neural circuit between the ventral midline thalamus nuclei and the basolateral amygdala (BLA) is activated²². Conversely, inactivation of the BLA silenced the fear behavior induced by the looming stimulus²⁵. The central amygdala (CeA) is also involved in defensive behaviors^{18,26}, notably through its neuronal connection to the PAG²⁷. In their study, Tovote and colleagues showed that CeA activation induces the disinhibition of the ventrolateral PAG (vlPAG) neurons, resulting in freezing behavior in mice. In contrast, dorsolateral PAG (dlPAG) escape-evoking neurons inhibit vlPAG neurons, thereby inducing a flight response. Therefore, the PAG appears to be a key structure for regulating fear behavior in response to threat. Finally, a recent study shows that the neuronal circuit between the hippocampus and the anterior hypothalamic nucleus controls the goal-directed escape toward a shelter²⁸.

Aging is often accompanied by profound behavioral changes, notably regarding locomotor activity and motor coordination, anxiety-like behaviors, auditory startle response, pain sensitivity, as well as spatial and working memory²⁹. For instance, the freezing response to auditory cues after Pavlovian fear conditioning is impaired in aged rodents^{29–31}. At the neurobiological level, aging is associated with numerous cellular alterations such as aberrant activity of neuronal network³² and cognitive impairments in aged rats have been linked to a decrease in functional brain connectivity³³. Brain structural changes also occur during aging, including morphological alterations of neuronal cells in the amygdala³⁴, increase of glial volume fraction in the superficial layers of the SC³⁵, as well as astrocytic alterations in the PAG³⁶. Thus, aging is characterized by a wide range of changes, from behavioral to cellular level. However, little is known about the impact of aging on innate fear behavior³⁷.

In the present study, we examine looming-evoked behaviors and cellular activity in brain regions involved in these defensive responses in young and aged mice.

Results

Behavioral response to looming stimuli changes with age

In order to investigate the innate fear response in young and old mice, we submitted animals to a looming stimulus which imitates a flying predator rapidly approaching the mouse from above (Fig. 1a).

Prior to testing the innate fear response, mice were first habituated to the setup. During this habituation session, we observed that aged mice moved a reduced distance, at a lower average speed (Supplementary Fig. S1a and b: distance moved, $p=0.0230$, mean speed, $p=0.0152$, Mann-Whitney tests). Thus, we calculated a ratio between the time spent in the central zone of the arena and the distance moved for each mouse to examine whether a lower time spent in the center is linked to the altered locomotion of aged mice or not. We showed that the ratio of the aged mice did not differ from the one of young mice (Supplementary Fig. S1c: ratio center time/distance moved, $p=0.2309$, unpaired t-test). This suggests that anxiety-like behaviors of aged mice are not altered, which is in line with the fact that aged mice did not spend a higher amount of time in the shelter than young mice (Supplementary Fig. S1d: shelter time, $p=0.0545$, Mann-Whitney test).

Only mice exposed to the looming stimulus expressed a fear response (i.e. escape and/or freezing). The control mice did not show any specific behavior as they explored the arena (Fig. 1b). The looming stimulus triggers a robust flight response to the shelter in most of the young mice (92%) (Fig. 1b). Interestingly in aged mice, we observed that 67% of them showed a predominant freezing behavior when confronted to the looming stimulus and only a third of them escaped toward the shelter. Noticeably, the latency to escape toward the shelter was higher in aged compared to young mice (Fig. 1c: escape latency in young, $n=11$ mice, 0.26s versus aged, $n=7$ mice, 6.27s, $p<0.0001$, Mann-Whitney test). A thorough analysis revealed that either young or aged mice in the control or looming conditions, accelerate when they reach the center of the arena (Fig. 1d and e, time=0s). Also, the speed of young mice increased immediately when the stimulus was triggered and the mice escaped (Fig. 1d). Then, the speed dropped rapidly, as the mice froze under the shelter (Fig. 1d). In contrast to young mice, the speed of aged mice decreased immediately after stimulus onset. Most of aged mice initially showed freezing behavior, after which two types of behavior could be distinguished, mice maintaining a freezing response with low speed (light purple, $n=14$) and mice escaping toward the shelter with high speed (dark purple, $n=7$) (Fig. 1e).

Overall, these data show that aged mice predominantly exhibit freezing behavior in response to innate fear triggered by visual threat, while a minority of them adopt delayed flight behavior.

Brain activity triggered in response to looming stimulus is impacted by age

Mice were sacrificed 90 min after the looming test, in order to target peak expression of the neuronal activity marker c-Fos. The density of c-Fos-immunopositive (c-Fos⁺) cells was estimated in ten brain regions of interest (Fig. 2a and b) and compared between home-cage, control and looming conditions for each age. Brain regions were selected according to their involvement in fear-evoked responses to a looming stimulus.

In young mice, a mixed-effects analysis was performed, revealing a significant influence for each factor and their interaction (Fig. 2c: condition effect $F_{(2,20)}=12.36$, $p=0.0003$, region effect $F_{(2,624,52,18)}=34.68$, $p<0.0001$, condition x region effect $F_{(18,179)}=5.148$, $p<0.0001$). Tukey's multiple comparisons test shows differences of c-Fos⁺ cell density between conditions in the amygdala, the dlPAG, the dorsal hippocampus and the LPTN. Indeed, we observed a significant increase of c-Fos⁺ cell density in the BLA, the CeA and the LA in the looming group compared to the home-cage animals (Fig. 2c: home-cage vs. looming, BLA, $p=0.0057$, CeA, $p=0.0283$, LA, $p=0.0093$). Only the increase in the BLA differs from that of the control group (Fig. 2c: control vs. looming, BLA, $p=0.0195$, CeA, $p=0.1535$, LA, $p=0.0607$). Noticeably, we observed a significant increase of c-Fos⁺ cell density in the dlPAG compared with the home-cage group, both under control and looming conditions (Fig. 2c: dlPAG, home-cage vs. control, $p=0.001$, home-cage vs. looming, $p=0.0001$). Furthermore, a considerable

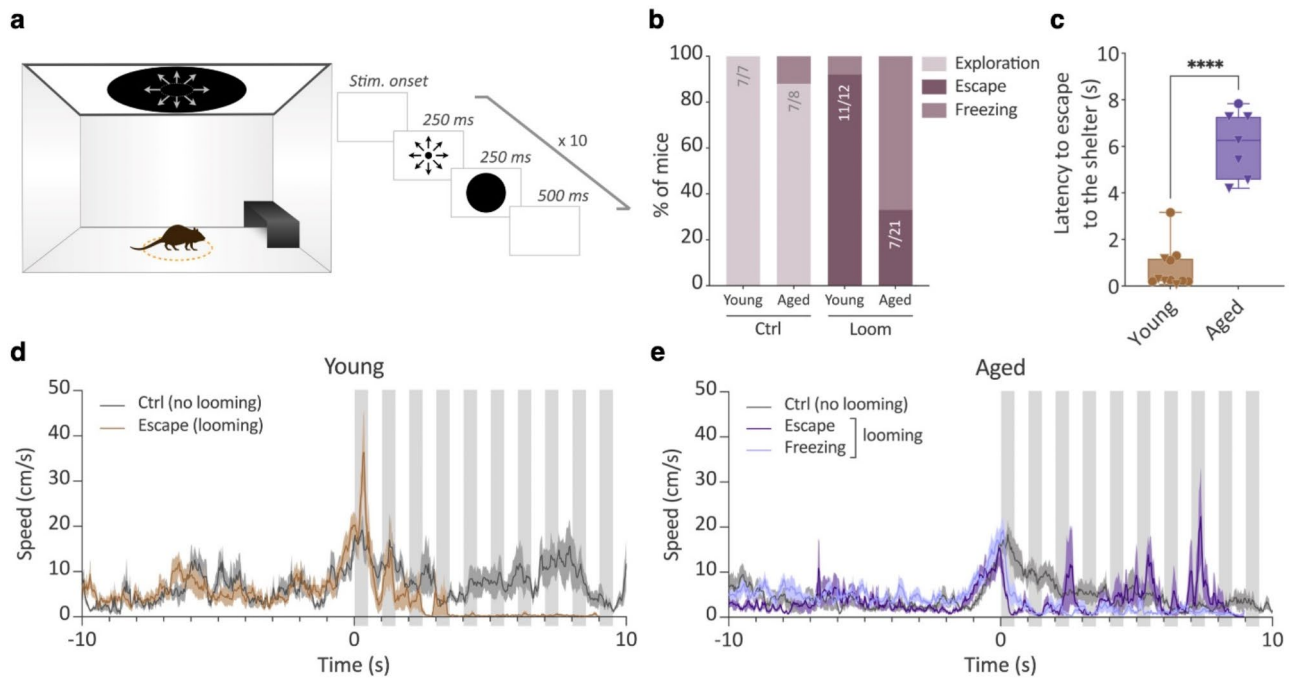


Fig. 1. Aged mice do not show robust escape behavior in response to looming stimulus. **(a)** Representation of the behavioral apparatus generating looming stimulus (left). The stimulus is presented when the mouse enters a virtual central zone (orange dotted circle) according to the indicated timing (right). **(b)** Percentage of young (3–4 months) and aged (23–25 months) mice in the “Control” (Ctrl) or “Looming” (Loom) conditions showing exploration or innate fear behavioral responses during looming stimulus. **(c)** Latency to escape to the shelter after stimulus onset for young ($n = 11$) and aged ($n = 7$) mice. Data are represented by the median (female and male mice are respectively represented by circles and triangles), **** $p < 0.0001$. Speed of young **(d)** and aged **(e)** mice in the “Control” (Ctrl, $n = 7$ young, $n = 8$ aged) or in the “Looming” ($n = 12$ young, $n = 21$ aged) groups for 10 s before (-10 to 0 s) and during (0 to 10 s) the stimulus. The performance of young and aged control mice is centered on their entry into the virtual central zone, even though the stimulus was not displayed for them. The performance of aged mice is displayed in 2 groups: animals showing only a freezing response (no escape behavior) (light purple, $n = 14$) and those showing both escape and freezing behavior (dark purple, $n = 7$). Each gray bar represents a looming stimulus, as shown in **a**. Data are represented as mean \pm SEM.

and significant increase of c-Fos⁺ cell density was observed in the dorsal hippocampus of control and looming animals, compared to the home-cage mice (Fig. 2c: home-cage vs. control, CA3, $p < 0.0001$, DG, $p < 0.0001$; home-cage vs. looming, CA3, $p = 0.0031$, DG, $p < 0.0001$). However, looming mice showed a significant decrease in c-Fos⁺ cell density in CA3 compared to control animals (Fig. 2c: CA3, control vs. looming, $p = 0.042$). We also highlighted a significant decrease of c-Fos⁺ cell density in the LPTN of looming mice compared with the control group (Fig. 2c: LPTN, control vs. looming, $p = 0.0396$). Besides, in a relevant proportion of young mice (5/12), looming was associated with a higher, but non-significantly different, c-Fos⁺ cell density in the PBGN compared to other groups (Fig. 2c: PBGN, home-cage vs. looming, $p = 0.269$, control vs. looming, $p = 0.1243$). Finally, we did not observe any significant change of cellular activity between conditions in the SC (Fig. 2c: SC, home-cage vs. control, $p = 0.1258$, home-cage vs. looming, $p = 0.1432$, control vs. looming, $p = 0.997$) or its upper layers (Fig. 2c: uSC, home-cage vs. control, $p = 0.8555$, home-cage vs. control, $p = 0.7337$, control vs. looming, $p = 0.9136$). Thus, exposure to the arena led to notable changes in brain cellular activity in young mice. In particular, these changes were observed in the amygdala, the dorsal hippocampus and the dIPAG, known to be involved in innate defensive behaviors^{18,22,25–28}. However, the looming stimulus triggers changes only in the BLA, CA3 region and LPTN.

For aged mice, a two-way ANOVA analysis reveals a significant effect of condition and brain region, but not of their interaction (Fig. 2d: condition effect $F_{(2,16)} = 5.063$, $p = 0.0198$, region effect $F_{(4,910, 78.56)} = 12.93$, $p < 0.0001$, condition \times region effect, $F_{(18,144)} = 0.9191$, $p = 0.5568$). The following Tukey’s post-hoc tests show only an increase of c-Fos⁺ cell density in the dIPAG and CA3 region of the looming animals compared to the home-cage group (Fig. 2d: dIPAG, home-cage vs. looming, $p = 0.0199$, CA3, home-cage vs. looming, $p = 0.0271$). Unlike young mice, exposure to the arena alone does not modify basal brain activity in aged mice (compared to home-cage), and the looming stimulus induces an increase in cellular activity only in rare brain regions (dIPAG, CA3). This suggests that there is an alteration in brain activation following the looming event in aged mice.

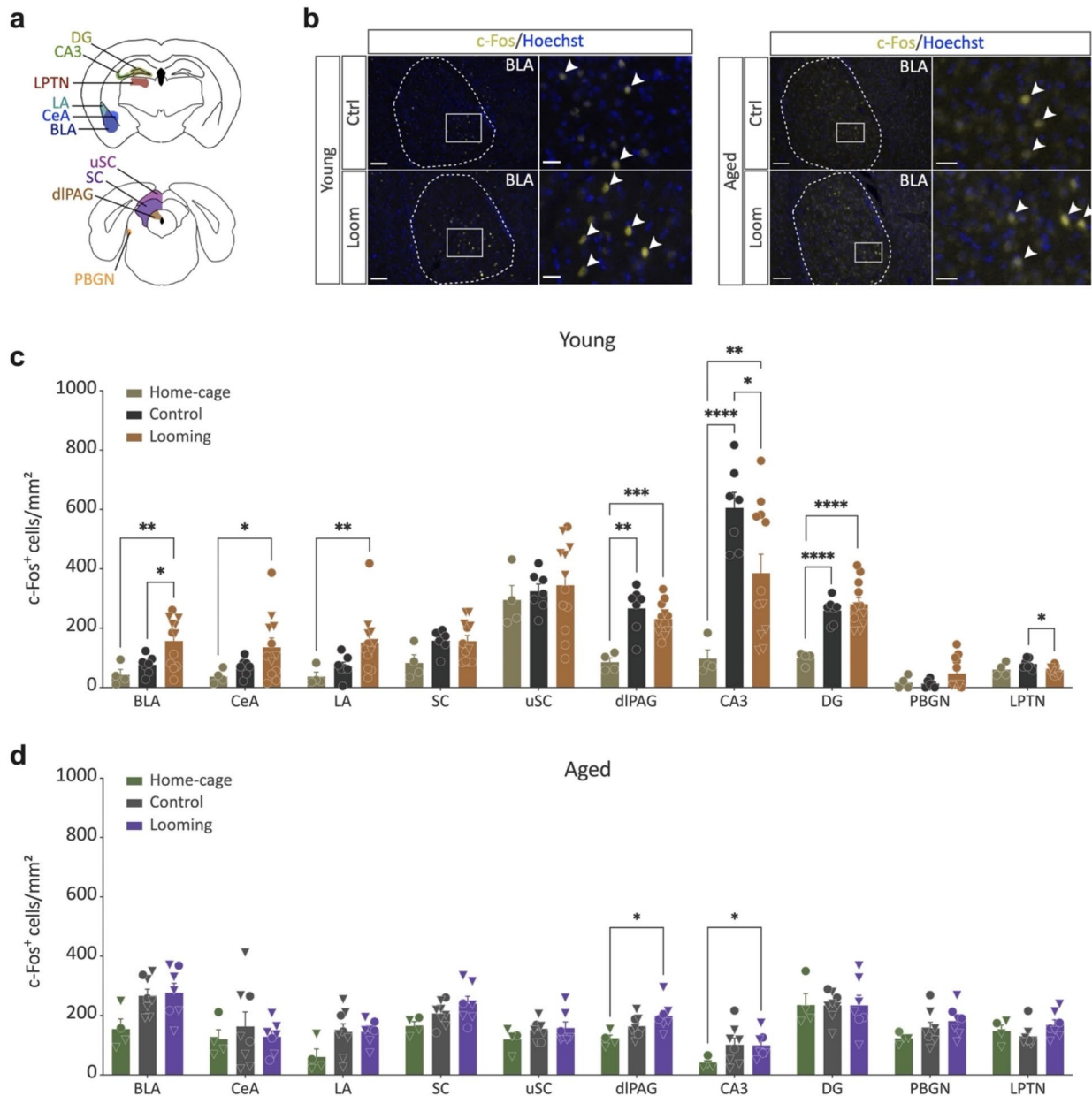


Fig. 2. C-Fos expression in various brain regions in response to looming stimulus in young and aged mice. **(a)** Schematic representation of brain structures selected for c-Fos immunohistochemistry analysis [Bregma - 1,82 (*top*) and - 4,16 mm (*bottom*)]. **(b)** Photomicrographs of brain sections following c-Fos immunohistochemistry and counterstaining with Hoechst. Arrows indicate the presence of c-Fos immunolabeled (c-Fos⁺) cells in the BLA of control (Ctrl) and looming (Loom) animals (scale bars = 100 μm/25 μm). Density analysis of c-Fos⁺ cells in the dentate gyrus (DG) and the CA3 region of the dorsal hippocampus, the basolateral (BLA), central (CeA) and lateral (LA) amygdala, the lateral posterior thalamic nucleus (LPTN), the superior colliculus (SC) and its upper layers (uSC), the dorsolateral periaqueductal gray (dlPAG) and the parabigeminal nucleus (PBGN) of **(c)** young mice in the “Home-Cage”, “Control” (*n* = 7) and “Looming” (*n* = 12) conditions and **(d)** aged mice in the “Home-Cage” (*n* = 4), “Control” (*n* = 8) and “Looming” (*n* = 7) groups (female and male are represented by circles and triangles, respectively). Data are represented as mean ± SEM; **p* < 0.05, ***p* < 0.01, ****p* < 0.001, *****p* < 0.0001 by Tukey’s post-hoc tests.

Looming stimulus recruits different brain networks depending on age

To investigate the neural networks involved in response to looming stimulus, we studied the functional connectivity between the 10 brain regions selected for c-Fos analysis by assessing the co-variation of c-Fos⁺ cell density for each pair of brain structures. We depicted the 45 correlations for each group using matrices (Figs. 3a

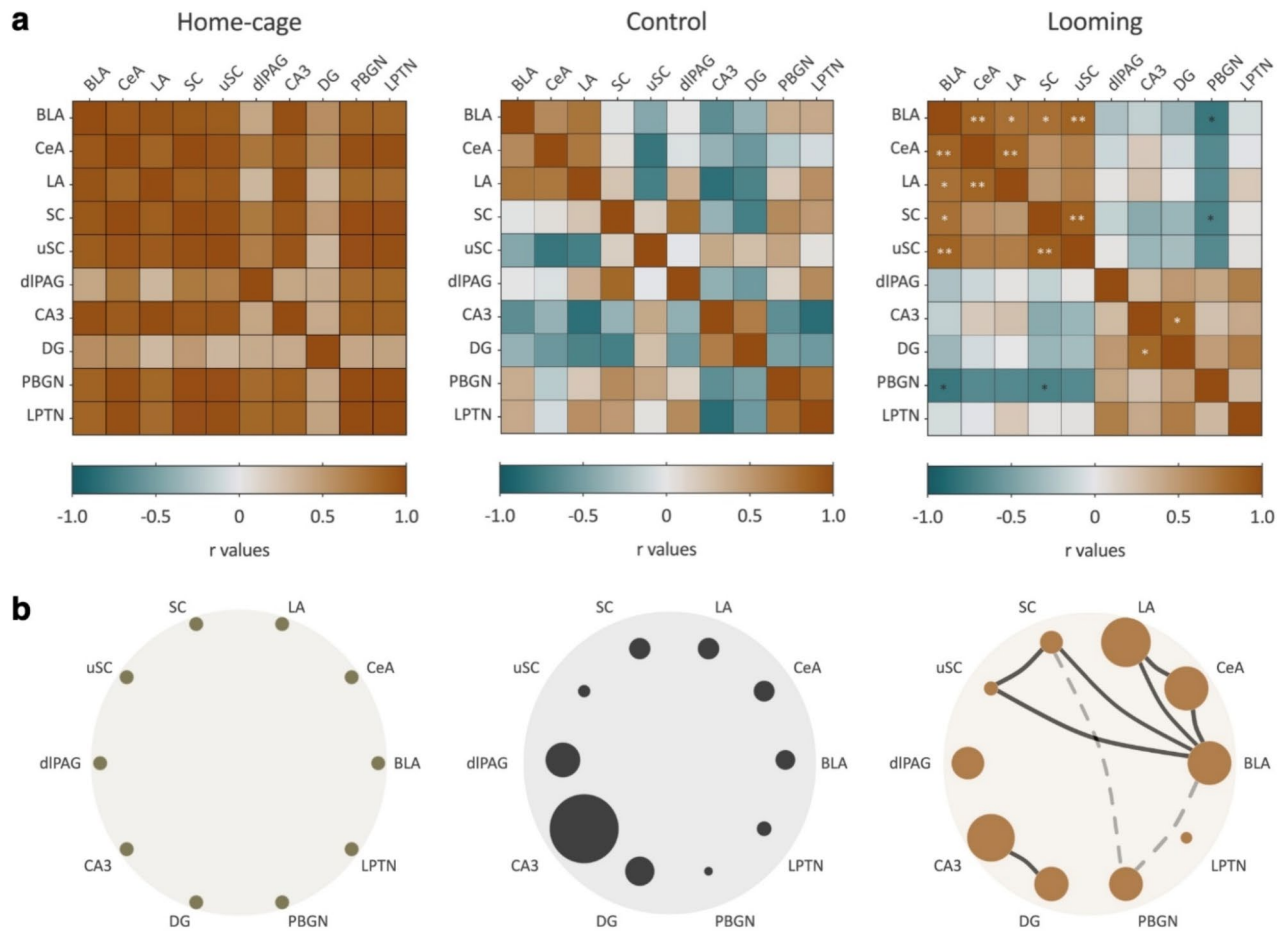


Fig. 3. Correlation matrices and functional brain connectivity networks recruited by looming stimulus in young mice. **(a)** Correlational analysis of *c-Fos* expression between brain regions of young animals in «Home-Cage», «Control» and «Looming» groups. The color of each box depicts Pearson's correlation coefficient (*r* values range from -1 to 1) according to the brain regions being compared. $*p < 0.05$, $**p < 0.01$. **(b)** The network representations for each correlation matrix show only significant positive (solid black lines) or negative (dashed gray lines) correlations. Each brain structure is plotted as a circle with a size representing the fold change in *c-Fos*⁺ cell density between experimental (Control and Looming) and Home-Cage conditions. Thickness of the link represents the *r* value of the correlation. LA (lateral amygdala), CeA (central amygdala), BLA (basolateral amygdala), LPTN (lateral posterior thalamic nucleus), PBGN (parabigeminal nucleus), DG (dentate gyrus of the dorsal hippocampus), CA3 (CA3 region of the dorsal hippocampus), dlPAG (dorsolateral periaqueductal gray), uSC (upper layers of superior colliculus), SC (superior colliculus).

and 4a) and networks (Figs. 3b and 4b). Significant correlations in the matrices are signaled by stars according to their *p*-values. The networks show only significant matrix correlations between the studied structures.

In young mice, only the looming group showed significant correlations between brain regions. Indeed, functional connectivity networks in response to the looming were observed, showing robust functional connections between the amygdalar nuclei (LA, BLA, CeA), the SC, and the PBGN (Fig. 3) which was expected, based on the anatomical connections between those 3 structures^{25,26}. This analysis shows that mice in the home-cage condition exhibit only positive correlations, while the control group tends to display more negative correlations. However, in both groups, none of the correlations were significant, preventing us from identifying a functional connectivity network.

In aged mice, the impact of context and impending stimulus on brain activity in the regions studied appears to be much weaker. Indeed, only the increased neuronal activation in dlPAG and CA3 is preserved in aged mice subjected to looming (compared to aged-matched home-cage), while activations in amygdala nuclei have disappeared (Fig. 2d). Unlike in young mice, no correlation patterns emerged in aged mice following the looming stimulus (Fig. 4), suggesting that functional brain connectivity in response to looming stimulus is altered with age.

Discussion

The aim of this study was to examine the impact of aging on innate defensive behavior in response to a looming stimulus and to determine whether these behavioral responses are associated with alterations in brain activity.

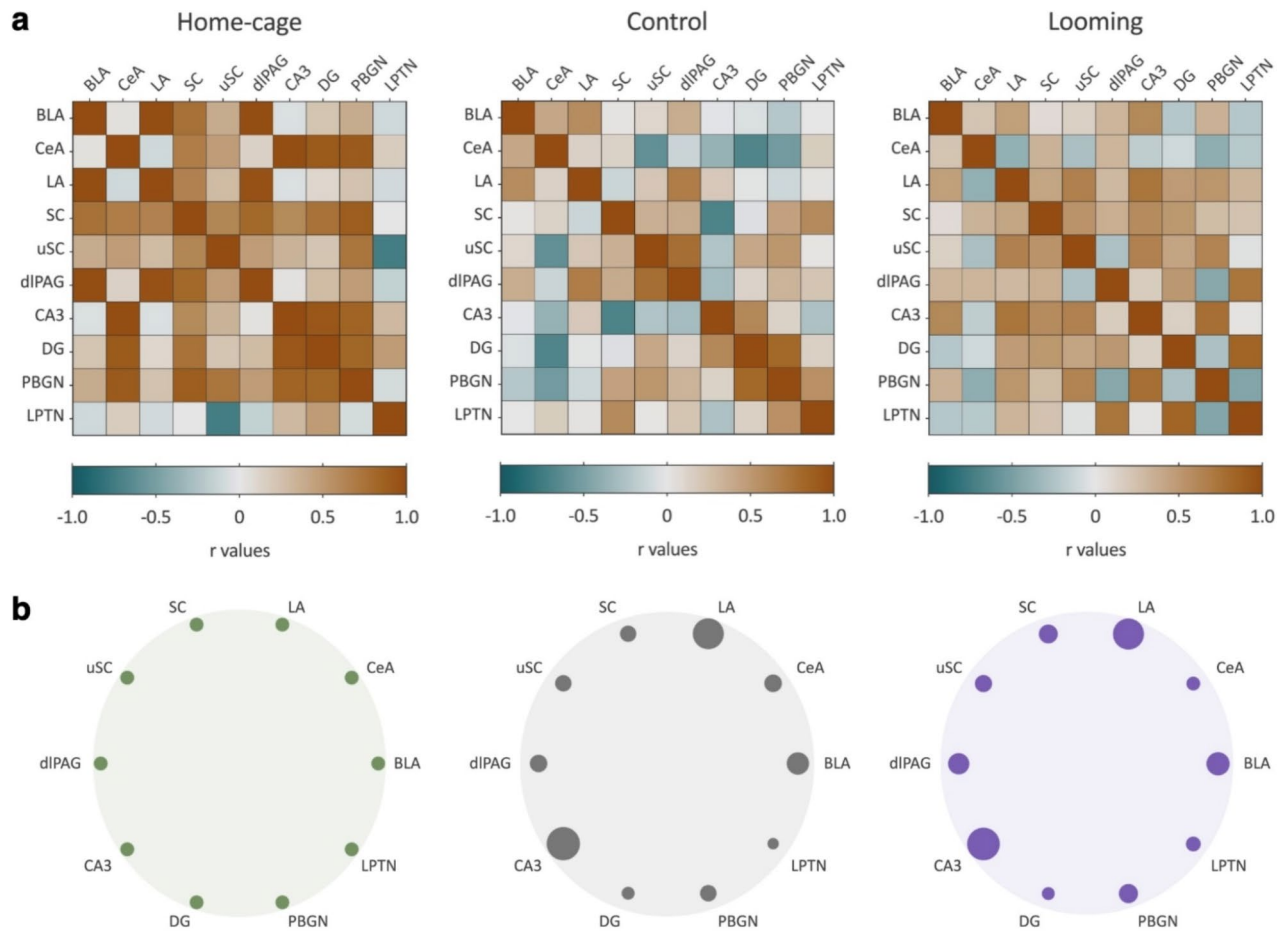


Fig. 4. Correlation matrices and functional brain connectivity networks recruited by looming stimulus in aged mice. **(a)** Correlational analysis of *c-Fos* expression between brain regions of aged mice in «Home-Cage», «Control» and «Looming» groups. The color of each box depicts the Pearson correlation coefficient (ranging from -1 to 1) according to the brain regions being compared. **(b)** The network representations for each correlation matrix only show significant correlations. Each brain structure is plotted as a circle with a size representing the fold change in *c-Fos*⁺ cell density between experimental (Control and Looming) and Home-Cage conditions. LA (*lateral amygdala*), CeA (*central amygdala*), BLA (*basolateral amygdala*), LPTN (*lateral posterior thalamic nucleus*), PBGN (*parabigeminal nucleus*), DG (*dentate gyrus of the dorsal hippocampus*), CA3 (*CA3 region of the dorsal hippocampus*), dlPAG (*dorsolateral periaqueductal gray*), uSC (*upper layers of superior colliculus*), SC (*superior colliculus*).

We found that most aged mice exhibit freezing behavior rather than escape when confronted with this visual threat stimulus, while young mice display a robust flight response. After stimulus presentation, old mice show an increase in *c-Fos*⁺ cell density only in the dlPAG and CA3 region, whereas young mice show changes in cell activity in the dorsal hippocampus (DG and CA3), amygdalar nuclei, LPTN and dlPAG. Additionally, functional brain connectivity in response to a looming stimulus is altered in aged mice.

In this study, we chose to individually-house the mice to reduce interindividual variability caused by the aggressive behavior observed more particularly in a group of aged mice, and favor a robust flight response to the looming stimulus³⁸. Social isolation is known to increase vigilance³⁹ and reactivity^{40,41}, which may contribute to the escape response in young mice. However, social isolation also leads to anxiety⁴². While our experiment did not reveal a difference on anxiety-like behavior in both young and aged mice, we cannot rule out the possibility of altered emotional behavior in aged mice⁴³, which could affect their fear response to the looming stimulus. In the future, this hypothesis could be tested by using anxiolytic or antidepressant substances, which are known to reduce freezing behavior following fear conditioning^{43,44}.

Another aspect to consider is that aging leads to a decline of visual acuity and contrast sensibility in C57Bl/6 mice⁴⁵. Although we can exclude a complete loss of vision in the aged mice - since all of them reacted to the looming stimulus (i.e. froze and/or escaped) - they may perceive the stimulus differently than young mice. It was reported that a less contrasted looming stimulus decreases the probability of escape in mice, as the stimulus becomes less salient²⁰. Thus, an altered perception of the looming stimulus due to decreased contrast sensitivity in aged mice may explain the change in their defensive behavioral response.

The effect of age on the response to a looming stimulus has been little studied. Liu and collaborators explored the looming-evoked response across the mouse lifespan and found no behavioral difference in 20 month-old mice³⁷. The discrepancy between their findings and ours may be due to differences in looming setups and the use of transient social isolation in our study, as they used group-housed mice.

At the functional level, we observed significant changes of cellular activation in numerous brain structures of young mice exposed to the looming stimulus. These changes led to the emergence of a pattern of functional connectivity between brain regions involved in innate fear responses. However, no functional connectivity signatures were observed in aged mice in response to looming. This is consistent with a previous study showing a decrease in brain functional connectivity in aged rats associated with cognitive deficits³³. Furthermore, it was shown that c-Fos expression decreases in the brain of aged rats⁴⁶ and that aging is coupled with excitation/inhibition imbalance⁴⁷. Taken together, this evidence could explain the loss of functional connectivity network and the modified behavioral response of old mice. In young mice, amygdalar nuclei (BLA, CeA and LA) were activated by the looming stimulus. This was expected given the fear response of mice to the visual stimulus, which is supported by activation of brain's fear pathways, in which the amygdala is a core structure²⁴. Furthermore, the BLA appears to be the central hub of the brain network activated by looming animals (Fig. 3a), as it is connected to other amygdalar nuclei (LA and CeA), as well as to the SC and its upper layers, and finally to the PBGN. The connection to the SC may be indirect, as the SC projects to the ventral midline thalamus, which in turn sends projections to the BLA and regulates behavioral responses to looming²². However, anatomical link with the PBGN has not been previously observed, despite the fact that this nucleus projects to the CeA²⁶. Given the crucial role of the BLA in the looming fear response^{25,48}, its central position is not surprising. In addition, we observed a non-significant increase of cell activity in PBGN and a significant decrease in LPTN in young mice. This co-occurrence could be correlated with the defensive behavior triggered by the stimulus. Indeed, activation of the SC-PBGN pathway leads to an escape response, while activation of the SC-LPTN induces freezing¹⁹. In this way, the observed escape response triggered by the looming stimulus could reflect the dominant activation of the PBGN and the inactivation of the LPTN. However, in aged mice, the stimulus fails to trigger the c-Fos⁺ cell activation pattern in the PBGN and the LPTN compared to young mice, suggesting an imbalance between these two brain pathways. The dIPAG activation was also present in aged mice. However, comparing the node size in the network representation between ages shows that this increase is less pronounced in old mice, which could be related to their lack of flight response. Finally, we observed increases of c-Fos labeling in the DG and CA3 of the dorsal hippocampus in young mice exposed to the arena and the looming stimulus. This cellular activation of dorsal hippocampal areas (DG and CA3) is likely related to the contribution of these regions to spatial context encoding⁴⁹. These changes in the DG are not found in aged mice, in line with known age-related alterations of hippocampal functions⁵⁰. Lack of brain activity in old mice has already been observed and correlated to poor memory performances after a recognition memory⁵¹. However, we did observe an increase of c-Fos labeling in the CA3 region of old mice, but this was weak compared to the increase seen in young mice.

In conclusion, our study reveals that aging affects the innate fear response to a threatening visual stimulus and recruits altered functional brain networks. Further investigations are needed to identify the brain mechanisms underlying defensive behavior to a looming stimulus in mice at different ages.

Methods

Animals

Young (3–4 months) and aged (23–25 months) adult C57Bl/6J female and male mice were used. Initially, mice were obtained from Janvier Labs (France) before being bred and maintained in the animal facility of the Center for Integrative Biology (CBI, Toulouse). Animals were housed in groups of four to six animals, at 23 °C with a 12-hour light-dark cycle (8:00 AM – 8:00 PM) with *ad libitum* access to water and food. All experiments were conducted in accordance with relevant guidelines and regulations, and approved by the French Ministry of Research and local ethic committees (APAFIS #12342-2017082111489451 v6 and #12343-2017111516096417 v9) and in compliance with the European directive 2010/63/UE. All methods used in this study conformed to the ARRIVE guidelines.

Looming test

Each animal was housed individually four days prior to the start of behavioral experiments to ensure a strong flight response to the looming stimulus³⁸. Animals were handled for 2 min during the two days preceding the behavioral test.

The apparatus (Imetronic, France) consisted of a rectangular arena (40 cm x 38 cm x 31 cm) containing an opaque shelter (12.5 cm x 10 cm x 4.5 cm). LCD monitor was placed on the ceiling to present visual stimuli.

The first day, each mouse was allowed to explore the arena and shelter freely during 10 min of habituation, without any stimulus. The next day, each animal was placed back in the arena for 5 min, after which, the mouse could trigger the looming stimulus by entering a virtual zone located in the center of the arena. The looming stimulus consisted of 10 repetitions of a black disc expanding from a diameter from 1 to 25 cm in 250 ms and remaining on the screen for another 250 ms. The stimulus was repeated with an intertrial interval of 500 ms (Fig. 1a). Mice innate fear response was measured during the 10 s of the looming stimulus. The setup was cleaned with 30% ethanol between each mouse.

All habituation and looming test sessions were recorded and analyzed using Ethovision XT 16 software (Noldus, Netherlands). Mice velocity, distance moved, and time spent in the different zones of the arena were measured. Freezing behavior was defined as an event lasting at least one second during which the mouse's speed was less than 15% of its average speed calculated over the 10 s preceding the stimulus¹⁰. Conversely, escape behavior was defined as an event in which the mouse reaches the shelter at a speed 4 times greater than its

average speed calculated over the 10 s preceding the stimulus. Each mouse was considered as freezing and/or escaping if it displays this behavior at least once.

Animals of “home-cage” group were not subjected to either the habituation session or the looming stimulus. Mice in the “control” group underwent the same habituation session as those in the “looming” group, but did not trigger the looming stimulus upon entering the virtual central area during the test day.

Tissue processing and c-Fos immunohistochemistry

C-Fos immunohistochemistry was performed on mice from the three experimental groups. Mice from the control and looming conditions were deeply euthanized with an intraperitoneal injection of high dose of pentobarbital (400 mg/ml, Euthasol vet, Dechra) and transcardially perfused (0.9% NaCl), 90 min after removal from the arena. As they were not exposed to the arena, mice from the home-cage condition were transcardially perfused in the morning of the test day. Brains were collected and post-fixed in paraformaldehyde solution (4% PFA) for 48 h before being stored in a 30% sucrose solution (containing 0.1% sodium azide). Then, 30 μ m-thick coronal sections were obtained using a cryomicrotome (Leica SM2010R, Leica Biosystems, Nanterre, France) and were stored in a cryoprotectant solution at -20 °C until use.

Series of 1/12 free-floating sections were then put through an immunostaining protocol against c-Fos. On day one, sections were washed in 0.1 M phosphate buffered saline containing 0.25% triton (PBST) and then placed in a solution containing 10% methanol and 10% H₂O₂ in PBST to block endogenous peroxidases. After a rinse with PBST, sections were incubated for 1 h in a blocking solution (10% NDS; 1% BSA; PBST). Finally, they were incubated in the blocking solution containing rabbit anti-c-Fos primary antibody (1/1000 ; Abcam ab190289 ; #GR3379960-1 ; #1026805-1) overnight at room temperature under agitation. The next day, the sections were rinsed in PBST before being incubated for 90 min in the blocking solution containing a fluorescent secondary antibody (Alexa 555 donkey anti-rabbit antibody ; 1/500 ; Life Tech A31572). Finally, the sections were rinsed and stained with Hoechst (1/10000) before being mounted on slides and coverslipped using a Mowiol medium.

Image acquisition and analysis

Images were obtained from these brain sections observed with a 10X objective of a fluorescence microscope (Leica DM6000 B, Leica, Nanterre, France) equipped with Mercator software (Explora Nova, La Rochelle, France).

Densities of c-Fos-immunopositive (c-Fos⁺) cells were estimated from images using Image J software. Briefly, cerebral structures outlines were manually traced on Hoechst images according to a mouse brain atlas⁵² and reported on c-Fos images where a fixed threshold was applied for each brain region. C-Fos⁺ cells were then counted using the “analyze particle” function for which we determined and set the parameters for each structure. The density of c-Fos⁺ cells was then calculated, so that each individual value represents the mean of measurements obtained from images acquired on three serial brain sections (separated by 360 μ m) of the same animal.

Statistical analysis

Statistical analysis was carried out using Prism 10 software. Due to the limited number of mice, males and females were grouped together in each experimental condition, and sex differences were not examined in this study.

Statistical analysis of behavior and c-Fos⁺ cell density

For behavioral analysis, the statistical significance was determined by a Mann-Whitney test for the latency to escape (during looming session), the distance moved and the speed (during habituation session). The ratio of the time spent in the central zone out of the total distance moved during the habituation session was analyzed by an unpaired t-test. For c-Fos⁺ cell density analysis, the statistical significance was assessed in young mice using a mixed effects analysis because the value of c-Fos⁺ cell density in the PBGN of one mouse was missing. For aged mice, a two-way ANOVA was performed with Geisser-Greenhouse correction. Each of these tests was followed by Tukey's multiple comparisons test to compare each condition within each brain region. Brain regions (BLA, CeA, LA, SC, uSC, dlPAG, CA3, DG, PBGN, LPTN) and conditions (home cage, control and looming) were used as variables in the mixed effects analysis and the two-way ANOVA. We were not able to compare c-Fos⁺ cell densities between young and aged mice since the immunohistochemistry experiments were carried on using 2 lots of antibodies against c-Fos (Abcam ab190289 ; #GR3379960-1 for young mice and Abcam ab190289 ; #1026805-1 for aged mice).

Inter-regional correlation analysis

Within each experimental group (“home-cage”, “control”, “young looming” and “aged looming”), Pearson correlation coefficients were determined for the pairwise comparisons of densities of c-Fos⁺ cells between all 10 studied brain areas. Benjamini-Hochberg corrections were used to control for false positive rates in multiple comparisons.

Network connectivity and correlation analysis

Calculations of Pearson correlation coefficients and densities of c-Fos⁺ cells were used to build network comparisons. Each brain region analyzed in this study was represented by a node, and the node size was proportional to the fold change of c-Fos density in a region of an experimental group compared to the same region in the “home-cage” group. The network connection lines show Pearson correlations between brain structures and were filtered to visualize correlations with a p-value < 0.05. Lines width relates to the r value of

the correlation between connected regions, a thick line denotes a high r value. The igraph package (igraph.org/r) in R (v1.2.4.1) was used to visualize the networks.

Data availability

The datasets generated and analysed during the current study are freely available from the corresponding author on request.

Received: 8 July 2024; Accepted: 17 October 2024

Published online: 25 October 2024

References

- Hennig, C. W., Dunlap, W. P. & Gallup, G. G. The effect of distance between predator and prey and the opportunity to escape on tonic immobility in *Anolis Carolinensis*. *Psychol. Rec.* **26**, 312–320 (1976).
- Dill, L. M. & Houtman, R. The influence of distance to refuge on flight initiation distance in the gray squirrel (*Sciurus carolinensis*). *Can. J. Zool.* **67**, 233–235 (1989).
- Liden, W. H., Phillips, M. L. & Herberholz, J. Neural control of behavioural choice in juvenile crayfish. *Proc. R. Soc. B.* **277**, 3493–3500 (2010).
- Domenici, P. Context-dependent variability in the components of fish escape response: Integrating locomotor performance and behavior. *J. Exp. Zool.* **313A**, 59–79 (2010).
- Temizer, I., Donovan, J. C., Baier, H. & Semmelhack, J. L. A visual pathway for looming-evoked escape in larval zebrafish. *Curr. Biol.* **25**, 1823–1834 (2015).
- Von Reyn, C. R. et al. Feature integration drives probabilistic behavior in the *Drosophila* escape response. *Neuron* **94**, 1190–1204e6 (2017).
- Zacarias, R., Namiki, S., Card, G. M., Vasconcelos, M. L. & Moita, M. A. Speed dependent descending control of freezing behavior in *Drosophila melanogaster*. *Nat. Commun.* **9**, 3697 (2018).
- De Haas, E. N. et al. The relation between fearfulness in young and stress-response in adult laying hens, on individual and group level. *Physiol. Behav.* **107**, 433–439 (2012).
- Papini, M. R., Penagos-Corzo, J. C. & Pérez-Acosta, A. M. Avian emotions: Comparative perspectives on fear and frustration. *Front. Psychol.* **9**, 2707 (2019).
- Yilmaz, M. & Meister, M. Rapid innate defensive responses of mice to looming visual stimuli. *Curr. Biol.* **23**, 2011–2015 (2013).
- Sagliano, L., Cappuccio, A., Trojano, L. & Conson, M. Approaching threats elicit a freeze-like response in humans. *Neurosci. Lett.* **561**, 35–40 (2014).
- Terburg, D. et al. The basolateral amygdala is essential for Rapid escape: A human and Rodent Study. *Cell* **175**, 723–735e16 (2018).
- Bhattacharyya, K., McLean, D. L. & MacIver, M. A. Visual threat assessment and reticulospinal encoding of calibrated responses in larval zebrafish. *Curr. Biol.* **27**, 2751–2762e6 (2017).
- Vale, R., Evans, D. A. & Branco, T. Rapid spatial learning controls instinctive defensive behavior in mice. *Curr. Biol.* **27**, 1342–1349 (2017).
- Silva, B. A., Gross, C. T. & Gräff, J. The neural circuits of innate fear: Detection, integration, action, and memorization. *Learn. Mem.* **23**, 544–555 (2016).
- De Franceschi, G., Vivattanasarn, T., Saleem, A. B. & Solomon, S. G. Vision guides selection of freeze or flight defense strategies in mice. *Curr. Biol.* **26**, 2150–2154 (2016).
- Huang, L. et al. A retinoraphe projection regulates serotonergic activity and looming-evoked defensive behaviour. *Nat. Commun.* **8**, 14908 (2017).
- Zhou, Z. et al. A VTA GABAergic neural circuit mediates visually evoked innate defensive responses. *Neuron* **103**, 473–488e6 (2019).
- Shang, C. et al. Divergent midbrain circuits orchestrate escape and freezing responses to looming stimuli in mice. *Nat. Commun.* **9**, 1232 (2018).
- Evans, D. A. et al. A synaptic threshold mechanism for computing escape decisions. *Nature* **558**, 590–594 (2018).
- Krout, K. E., Loewy, A. D., Westby, G. W. M. & Redgrave, P. Superior colliculus projections to midline and intralaminar thalamic nuclei of the rat. *J. Comp. Neurol.* **431**, 198–216 (2001).
- Salay, L. D., Ishiko, N. & Huberman, A. D. A midline thalamic circuit determines reactions to visual threat. *Nature* **557**, 183–189 (2018).
- Li, L. et al. Stress accelerates defensive responses to looming in mice and involves a locus coeruleus-superior colliculus projection. *Curr. Biol.* **28**, 859–871e5 (2018).
- LeDoux, J. E. Emotion circuits in the brain. *Annu. Rev. Neurosci.* **23**, 155–184 (2000).
- Wei, P. et al. Processing of visually evoked innate fear by a non-canonical thalamic pathway. *Nat. Commun.* **6**, 6756 (2015).
- Shang, C. et al. A parvalbumin-positive excitatory visual pathway to trigger fear responses in mice. *Science* **348**, 1472–1477 (2015).
- Tovote, P. et al. Midbrain circuits for defensive behaviour. *Nature* **534**, 206–212 (2016).
- Bang, J. Y. et al. Hippocampal-hypothalamic circuit controls context-dependent innate defensive responses. *eLife* **11**, e74736 (2022).
- Shoji, H. & Miyakawa, T. Age-related behavioral changes from young to old age in male mice of a C57 BL/6J strain maintained under a genetic stability program. *Neuropsychopharmacol. Rep.* **39**, 100–118 (2019).
- Gould, T. & Feiro, O. Age-related deficits in the retention of memories for cued fear conditioning are reversed by galantamine treatment. *Behav. Brain Res.* **165**, 160–171 (2005).
- Moyer, J. R. & Brown, T. H. Impaired trace and contextual fear conditioning in aged rats. *Behav. Neurosci.* **120**, 612–624 (2006).
- Mattson, M. P. & Arumugam, T. V. Hallmarks of brain aging: Adaptive and pathological modification by metabolic states. *Cell Metabol.* **27**, 1176–1199 (2018).
- Ash, J. A. et al. Functional connectivity with the retrosplenial cortex predicts cognitive aging in rats. *Proc. Natl. Acad. Sci. U.S.A.* **113**, 12286–12291 (2016).
- Von Halbach, B., Unsicker, K. & O. & Morphological alterations in the amygdala and hippocampus of mice during ageing. *Eur. J. Neurosci.* **16**, 2434–2440 (2002).
- Díaz, F., Moreno, P., Villena, A., Vidal, L. & De Pérez, I. Effects of aging on neurons and glial cells from the superficial layers of the superior colliculus in rats. *Microsc. Res. Tech.* **62**, 431–438 (2003).
- Jaworska-Adamu, J., Krawczyk, A., Rycerz, K. & Krawczyk-Marć, I. Age-related astrocytic changes in the periaqueductal gray matter (PAG) in rats. *Med. Weter* (2014).
- Liu, X. et al. Male and female mice display consistent lifelong ability to address potential life-threatening cues using different post-threat coping strategies. *BMC Biol.* **20**, 281 (2022).
- Lenzi, S. C. et al. Threat history controls flexible escape behavior in mice. *Curr. Biol.* **32**, 2972–2979e3 (2022).

39. Williams, J. B. et al. A model of Gene-Environment Interaction reveals altered mammary gland gene expression and increased tumor growth following social isolation. *Cancer Prev. Res.* **2**, 850–861 (2009).
40. Siegfried, B., Alleva, E., Oliverio, A. & Puglisi-Allegra, S. Effects of isolation on activity, reactivity, excitability and aggressive behavior in two inbred strains of mice. *Behav. Brain. Res.* **2**, 211–218 (1981).
41. Zelikowsky, M. et al. The neuropeptide Tac2 controls a distributed brain state induced by chronic social isolation stress. *Cell* **173**, 1265–1279e19 (2018).
42. Ieraci, A., Mallei, A. & Popoli, M. Social isolation stress induces anxious-depressive-like behavior and alterations of neuroplasticity-related genes in adult male mice. *Neural Plast.* 1–13 (2016).
43. Conti, L. H., Maciver, C. R., Ferkany, J. W. & Abreu, M. E. Footshock-induced freezing behavior in rats as a model for assessing anxiolytics. *Psychopharmacology* **102**, 492–497 (1990).
44. Inoue, T., Kitaichi, Y. & Koyama, T. SSRIs and conditioned fear. *Prog. Neuropsychopharmacol. Biol. Psychiatry* **35**, 1810–1819 (2011).
45. Lehmann, K., Schmidt, K. F. & Löwel, S. Vision and visual plasticity in ageing mice. *Restor. Neurol. Neurosci.* **30**, 161–178 (2012).
46. Lee, Y. I., Park, K. H., Baik, S. H. & Cha, C. I. Attenuation of c-Fos basal expression in the cerebral cortex of aged rat. *NeuroReport* **9**, 2733–2736 (1998).
47. Wong, T. P. et al. Imbalance towards inhibition as a substrate of aging-associated cognitive impairment. *Neurosci. Lett.* **397**, 64–68 (2006).
48. Khalil, V. et al. Subcortico-amygdala pathway processes innate and learned threats. *eLife* **12**, e85459 (2023).
49. Moser, M. B. & Moser, E. I. Distributed encoding and retrieval of spatial memory in the hippocampus. *J. Neurosci.* **18**, 7535–7542 (1998).
50. Rosenzweig, E. S. & Barnes, C. A. Impact of aging on hippocampal function: Plasticity, network dynamics, and cognition. *Prog. Neurobiol.* **69**, 143–179 (2003).
51. Belblidia, H. et al. Characterizing age-related decline of recognition memory and brain activation profile in mice. *Exp. Gerontol.* **106**, 222–231 (2018).
52. Paxinos, G. & Franklin, K. B. J. *The Mouse Brain in Stereotaxic Coordinates* (Academic, 2001).

Acknowledgements

We thank Virginie Bourlier (I2MC, Toulouse) for providing us full access to fluorescent microscopy. We also thank the CBI-ANEXPLO mice facility for animal care and the CBI-Mouse Behavioral Core (MBC) for behavioral support.

Author contributions

C.B., C.R. and C.F. conceptualized these experiments; C.B. and S.G. performed the behavioral experiments; C.B. and A.B. performed image acquisition and analysis; C.B. and C.L. performed immunohistochemistry experiments; C.B. analyzed all the data and drafted the manuscript. C.B., C.R. and C.F. reviewed and edited the final version of the manuscript.

Funding

This study was supported by grants from the Centre National de la Recherche Scientifique (CNRS, France) and the University of Paul Sabatier Toulouse 3 (UT3, France).

Declarations

Competing interests

The authors declare no competing interests.

Additional information

Supplementary Information The online version contains supplementary material available at <https://doi.org/10.1038/s41598-024-76884-y>.

Correspondence and requests for materials should be addressed to C.F.

Reprints and permissions information is available at www.nature.com/reprints.

Publisher's note Springer Nature remains neutral with regard to jurisdictional claims in published maps and institutional affiliations.

Open Access This article is licensed under a Creative Commons Attribution-NonCommercial-NoDerivatives 4.0 International License, which permits any non-commercial use, sharing, distribution and reproduction in any medium or format, as long as you give appropriate credit to the original author(s) and the source, provide a link to the Creative Commons licence, and indicate if you modified the licensed material. You do not have permission under this licence to share adapted material derived from this article or parts of it. The images or other third party material in this article are included in the article's Creative Commons licence, unless indicated otherwise in a credit line to the material. If material is not included in the article's Creative Commons licence and your intended use is not permitted by statutory regulation or exceeds the permitted use, you will need to obtain permission directly from the copyright holder. To view a copy of this licence, visit <http://creativecommons.org/licenses/by-nc-nd/4.0/>.

© The Author(s) 2024